



**HAL**  
open science

## Molecular characterisation of a cellular conveyor belt in *Clytia medusae*

Thomas Condamine, Muriel Jager, Lucas Leclère, Corinne Blugeon, Sophie Lemoine, Richard R Copley, Michaël Manuel

► **To cite this version:**

Thomas Condamine, Muriel Jager, Lucas Leclère, Corinne Blugeon, Sophie Lemoine, et al.. Molecular characterisation of a cellular conveyor belt in *Clytia medusae*. *Developmental Biology*, 2019, 456 (2), pp.212-225. 10.1016/j.ydbio.2019.09.001 . hal-02381895

**HAL Id: hal-02381895**

**<https://hal.science/hal-02381895>**

Submitted on 26 Nov 2019

**HAL** is a multi-disciplinary open access archive for the deposit and dissemination of scientific research documents, whether they are published or not. The documents may come from teaching and research institutions in France or abroad, or from public or private research centers.

L'archive ouverte pluridisciplinaire **HAL**, est destinée au dépôt et à la diffusion de documents scientifiques de niveau recherche, publiés ou non, émanant des établissements d'enseignement et de recherche français ou étrangers, des laboratoires publics ou privés.

# Molecular characterisation of a cellular conveyor belt in *Clytia* medusae

Thomas Condamine<sup>a</sup>, Muriel Jager<sup>a</sup>, Lucas Leclère<sup>b</sup>, Corinne Blugeon<sup>c</sup>, Sophie Lemoine<sup>c</sup>,  
Richard R. Copley<sup>b</sup>, Michaël Manuel<sup>a</sup>

<sup>a</sup> Sorbonne Université, MNHN, CNRS, EPHE, Institut de Systématique, Evolution, Biodiversité (ISYEB UMR 7205), Paris, France

<sup>b</sup> Sorbonne Université, CNRS, Laboratoire de Biologie du Développement de Villefranche-sur-mer (LBDV) UMR7009, 181 chemin du Lazaret, 06230, Villefranche-sur-mer, France.

<sup>c</sup> Genomic Paris Centre, Institut de biologie de l'Ecole normale supérieure (IBENS), Ecole normale supérieure, CNRS, INSERM, PSL Université Paris 75005 Paris, France.

Declarations of interest: none.

## ABSTRACT

The tentacular system of *Clytia hemisphaerica* medusa (Cnidaria, Hydrozoa) has recently emerged as a promising experimental model to tackle the developmental mechanisms that regulate cell lineage progression in an early-diverging animal phylum. From a population of proximal stem cells, the successive steps of tentacle stinging cell (nematocyte) elaboration, are spatially ordered along a "cellular conveyor belt". Furthermore, the *C. hemisphaerica* tentacular system exhibits bilateral organisation, with two perpendicular polarity axes (proximo-distal and oral-aboral). We aimed to improve our knowledge of this cellular system by combining RNAseq-based differential gene expression analyses and expression studies of Wnt signalling genes. RNAseq comparisons of gene expression levels were performed (i) between the tentacular system and a control medusa deprived of all tentacles, nematogenic sites and gonads, and (ii) between three samples staggered along the cellular conveyor belt. The behaviour in these differential expression analyses of two reference gene sets (stem cell genes; nematocyte genes), as well as the relative representations of selected gene ontology categories, support the validity of the cellular conveyor belt model. Expression patterns obtained by *in situ* hybridisation for selected highly differentially expressed genes and for Wnt signalling genes are largely consistent with the results from RNAseq. Wnt signalling genes exhibit complex spatial deployment along both polarity axes of the tentacular system, with the Wnt/ $\beta$ -catenin pathway probably acting along the oral-aboral axis rather than the proximo-distal axis. These findings reinforce the idea that, despite overall radial symmetry, cnidarians have a full potential for elaboration of bilateral structures based on finely orchestrated deployment of an ancient developmental gene toolkit.

*Keywords:* bilateral symmetry; cellular conveyor belt; Cnidaria; development; evolution; medusa; stem cells; tentacle; Wnt

## 1. Introduction

Cellular conveyor belts are defined as structures in which processes of cell proliferation and differentiation take place with clear spatial sorting of cellular stages along a polarity axis. Stem cells and actively dividing progenitors are localised at one pole, and differentiated cells at the opposite pole (Devès and Bourrat, 2012). Such systems are ideally configured for investigating mechanisms that regulate cell proliferation, cell cycle exit and differentiation. Their main practical advantage is that it is possible to infer the temporal sequence of transcriptional activation of genes from the spatial distribution of their expression domains along the cellular conveyor belt axis (Candal et al., 2004; 2007, Devès and Bourrat, 2012). Cellular conveyor belts are also promising models to uncover mechanisms that couple progression along a cell lineage, regulation of growth and tissue size, and polarity at the cell and tissue scales (Coste et al., 2016). Examples of cellular conveyor belts that have been investigated in vertebrates (illustrated in Devès and Bourrat, 2012) include the intestinal crypt of mammals, the retina of teleost fishes and amphibians, and the developing optic tectum in fish. Among non-vertebrate bilaterians, cellular conveyor belts have been observed, for instance, in developing optic lobes of flies (Joly et al., 2016) and cerebral ganglia of snails (Zakharov et al., 1998), and during neurogenesis at the ventral midline in the trochophore larvae of an annelid (Demilly et al., 2013).

Among non-bilaterian metazoans, there are only two well-documented instances of cellular conveyor belts: the tentacle root of ctenophores (best characterised in the species *Pleurobrachia pileus*, Alié et al., 2011; Dayraud et al., 2012; Jager et al., 2013) and the tentacle bulb of the hydrozoan cnidarian medusae (Denker et al., 2008; Jager et al., 2011; Leclère et al., 2012; Coste et al., 2016). These systems are uniquely suited to investigate the early evolution in metazoans of regulatory mechanisms orchestrating cell proliferation, cell cycle control and progression towards differentiation. In cnidarians, these mechanisms have mainly been studied in the hydra polyp, which is also characterised by spatially ordered tissue dynamics. In this system, cell divisions occur in the mid region of the body column and epithelia move continuously towards both extremities, where they are sloughed off (Campbell 1967 Dev. Biol., Bode 1996). The hydra polyp, however, does not fall within our definition of a conveyor belt, as cellular differentiation stages (e.g., of nematocytes) are not orderly distributed along the oral-aboral axis but are mixed up in the polyp body column, before late differentiation stages migrate to their final destination (e.g., foot or tentacles) (Bode 1996).

The tentacular system of the *Clytia hemisphaerica* medusa, which is the focus of the present study, comprises two distinct regions along a proximo-distal axis, the sub-spherical tentacle bulb, and the tentacle itself (Fig. 1A, B). The tentacle bulb ectoderm is the production site of cells that make up tentacle tissues, ensuring their continuous renewal. There is a high turnover of tentacle surface cells directly involved in prey catching, i.e. the single-use stinging cells or nematocytes. This cell type represents a unique evolutionary acquisition (synapomorphy) of the phylum Cnidaria, the likely sister-group of Bilateria (Simion et al., 2017). Monitoring of BrdU or EdU-labelled nuclei, analyses of serial histological sections, and gene expression studies, have demonstrated that production of nematocytes (nematogenesis) is a polarised process. Putative stem cells are located at the proximal pole of the bulb, and nematoblast differentiation progresses towards the distal pole, where nematocytes mature before reaching the tentacle (Fig. 1A). Stem cell marker genes such as *Piwi*, *Vasa*, *PL10* and *Nanos1* are expressed at the proximal pole of the tentacle bulb ectoderm in two lateral symmetrical patches connected (on the oral side) by a thin transverse line (Fig. 1A; Denker et al., 2008; Leclère et al., 2012). Proliferating progenitors occur throughout the bulb ectoderm, except in its distal-most region, and are absent in the tentacle (Denker et al., 2008; Coste et al., 2016). Cells expressing the *mcol3-4a* gene (a marker of nematoblast differentiation encoding a protein of the nematocyte capsule) are present at very high density in the intermediate part of the nematogenic bulb ectoderm, and at much lower density in the bulb tip and tentacle base, but they are absent from the rest of the tentacle and from the most proximal part of the bulb ectoderm (Denker et al., 2008). NOWA, a marker of late nematoblast differentiation, is highly expressed in the distal half of the bulb and in a few scattered cells of the tentacle base (Denker et al., 2008). Cellular stages are only imperfectly sorted, but according to counts on serial transverse sections, the ratio between early and late differentiation stages decreases progressively from proximal to distal (Denker et al., 2008).

In recent years, the advantages of the *C. hemisphaerica* nematogenic cellular conveyor belt as an experimental system have triggered several studies focusing on the early evolution of molecular processes that regulate animal development and tissue homeostasis. The localised expression of the so-called "germ line genes" (*Piwi*, *Vasa*, *PL10*, *Nanos*) at the proximal pole of the tentacle bulb (Denker et al., 2008; Leclère et al., 2012) has contributed to the realisation that in early metazoan history, these RNA regulators were playing roles in stem cell regulation rather than being specific to the germ line, a conclusion also supported by data

from Ctenophora (Alié et al., 2011), Porifera (Alié et al., 2015) and other hydrozoans such as *Hydra* (Mochizuki et al. 2000, 2000; Hemmrich et al. 2012, Juliano et al. 2014) and *Hydractinia* (Müller et al. 2004; Bradshaw et al. 2015). A case study focused on transcription factors of the Sox family has substantiated the interest of the *C. hemisphaerica* tentacle bulb for sorting out paralogues that in the context of nematogenesis are expressed in early vs. late stages of cellular lineage progression (Jager et al. 2011). Using an antibody directed against *C. hemisphaerica* Yorkie, Coste et al. (2016) observed spatial correlation between nuclear vs. cytoplasmic localisation of this protein, and presence vs. absence of cell proliferation, suggesting ancient conservation of a role of the Hippo pathway in the developmental arrest of cell proliferation.

However, the potential of the *C. hemisphaerica* tentacular system as an experimental model is currently impaired by a critical lack of fundamental knowledge. The nematogenic cellular conveyor belt is poorly characterised at the molecular level, with expression data published for only a handful of genes (Denker et al. 2008, Hwang et al. 2010, Jager et al. 2011, Leclère et al. 2012, Steinmetz et al. 2012, Coste et al. 2016, Leclère et al. 2019). In addition, previous studies have focused almost exclusively on nematogenesis, although the tentacular system also involves other cell types (such as epithelio-muscular cells, ganglion cells, sensory cells) as well as the underlying endoderm. Furthermore, the tentacular system has been interpreted only in terms of proximo-distal polarity, but in fact this structure also displays oral-aboral polarity, and therefore, bilateral symmetry. The oral pole of the tentacle bulb faces the subumbrellar side of the medusa, and the aboral pole the exumbrellar side (Fig. 1B). The oral-aboral axis, as in all cnidarians, is the primary body axis of the medusa. With respect to the process of nematogenesis, both polarity axes are relevant: the proximo-distal axis, because of the spatial ordering of cellular stages, and the oral-aboral axis, because the whole oral ectoderm is nematogenic, whereas the aboral side comprises a triangular shaped region of non-nematogenic ectoderm, extending along the midline (Denker et al., 2008).

Here we adopted two different, complementary approaches to improve our molecular understanding of the tentacular system of the *C. hemisphaerica* medusa: global comparison of gene expression along the proximo-distal axis by RNAseq, and expression analyses focused on Wnt signalling ligands and receptors. For the first approach, we performed differential gene expression (DGE) analyses between three samples representing successive areas along the proximo-distal axis of the tentacular system: (i) the proximal half of the tentacle bulb, (ii)

the distal half of the tentacle bulb + most proximal part of the tentacle (iii) the rest of the tentacle. We also compared whole tentacular systems to medusae deprived of all nematogenic zones (i.e. tentacle bulbs and tentacles, as well as the manubrium) and gonads (because the latter were expected to share many transcripts with tentacle-bulb stem cells). These RNAseq datasets are expected to serve as resources to enhance future in-depth studies of cellular and molecular processes using this experimental system. The DGE analyses presented here were mainly aimed at checking if the global behaviour of various functional categories of genes (such as stem cell genes, genes encoding structural components of the nematocyte capsule, and selected gene ontology (GO) categories) meet expectations from the cellular conveyor belt model. In addition, we performed experimental validation of the RNAseq DGE results by examining consistency with expression patterns obtained by *in situ* hybridisation (ISH) for selected highly differentially expressed genes.

This approach was complemented by a candidate gene expression study focusing on Wnt signalling genes. These are of special interest in the context of the medusa tentacular system primarily because Wnt signalling is a critical actor in the regulation of animal development (Garcin and Habib, 2017), stem cell self-renewal and cell proliferation (Sokol, 2011; Kühl and Kühl, 2013), cell fate specification and neurogenesis (Mulligan and Cheyette, 2012; Bielen and Houart, 2014; Noelanders and Vleminckx, 2017). Another facet of Wnt signalling of particular relevance here is its role in establishing and maintaining spatial polarities, in cnidarians as well as in other metazoans, at all scales from planar cell polarity to local (within organs) polarities and to whole body polarity axes (Lapébie et al., 2009; 2011; 2014; Momose et al., 2012; Loh et al., 2016; Sokol, 2015). Notably, the Wnt/ $\beta$ -catenin pathway has a highly conserved role in the establishment of the primary body axis (oral-aboral in cnidarians; antero-posterior in bilaterians), through a conserved oral/posterior Wnt-secreting centre thought to date back to a common ancestor of all Metazoa (Guder et al., 2006a; Momose et al., 2008; Ryan and Baxevanis, 2007; Petersen and Reddien, 2009; Niehrs, 2010; Marlow et al., 2013; Leininger et al., 2014). Our expression analyses reveal a complex spatial deployment of the various examined Wnt signalling genes along both polarity axes of the tentacular system, which for the first time helps to integrate the nematogenic cellular conveyor belt into its bilateral anatomical context.

## 2. Results and Discussion

### 2.1. Experimental design and definition of differential gene expression profiles

Two RNAseq experiments were performed (Fig.1A). In experiment A, gene expression was compared between three samples corresponding to successive regions along the proximo-distal axis of the tentacular system: peripheral area of umbrella + proximal half of the bulb (sample A1); distal half of the bulb + proximal portion of tentacle (sample A2); mature tentacle (sample A3). Experiment B involved comparisons of gene expression between the whole tentacular system (sample B2) and control medusae deprived of tentacle bulbs and tentacles, manubrium and gonads (for justification and details see Materials and Methods). These control medusae (sample B1) do contain some differentiated nematocytes (notably along the umbrella periphery and in the exumbrella epidermis) but at low density, but the important point is that they are devoid of all known areas of nematogenesis.

For differential analyses of gene expression in experiment A, a fold change  $\log_2(\text{FC})$  value  $> 2$  and an adjusted p-value ( $p\text{-adj}$ )  $< 0.05$  were used as thresholds to consider that a transcript is differentially expressed between two samples. Although all pairwise comparisons between these samples were performed, we will focus on 8 particular profiles of differential gene expression along the proximo-distal axis of the tentacular system. These profiles are graphically represented in Fig. 2, with different shades of grey between samples meaning statistically significant DGE, and darker tones representing higher expression levels. These graphical summaries of the pre-defined profiles only reflect the way they were defined. They must not be mistaken as depictions of the spatial distribution of transcripts (expression patterns) in the tentacular system. For example, a gene with an expression level higher in sample A1 with respect to A2 and A3 (Prox[1>2, 3]) may be restricted even within the bulb proximal half; furthermore its expression domain need not be restricted to the proximal half but may extend within the distal bulb half and tentacle as well.

These 8 expression profiles encompass all genes for which at least two of the pairwise comparisons between samples A1, A2 and A3 were statistically significant (Fig. 2). They are classified as follows: genes with higher expression in the proximal part of the bulb (close to the umbrella) than in the tentacle (“Prox”), genes with highest (“Mid”) or lowest (“Ext”) expression in the intermediate sample (sample A2), and genes with expression in the tentacle

higher than in the proximal half of the bulb (“Dist”). Six of the eight expression profiles correspond to situations in which a gene is over-expressed or under-expressed in one of the samples with respect to the two others (between brackets, "1, 2 and 3" stand for samples A1, A2 and A3): Prox[1>2,3], Prox[1,2>3], Mid[1<2>3], Dist[1<2,3], Dist[1,2<3] and Ext[1>2<3]). The profiles Prox[1>2>3] and Dist[1<2<3] are characterised by two sequential statistically significant differences in expression level along the axis of the tentacular system. These 8 expression profiles altogether comprised 27,582 genes (of 79,614 total genes). The remaining genes, which did not fall into any of the previous categories, are designated "others". They include some differentially expressed genes, but with statistically significant difference for only one of the three pairwise comparisons. These "other" genes cannot be qualified as differentially expressed at the scale of the whole proximo-distal axis of the tentacular system.

Results of experiment A were analysed either as such (“unfiltered”), or retaining only the genes that in experiment B are more strongly expressed in the tentacular system (B2) than in the control medusae (B1) (thereafter, “filtered” results of experiment A; Fig. 1A). Our threshold on FC with experiment B (cut-off values  $FC > 1$  and  $p\text{-adj} < 0.05$ ) is relatively non stringent, because these data were used to apply a filter on those of experiment A, to get rid of genes whose high expression levels in sample A1 are attributable to peripheral umbrella (rather than to tentacle bulb proximal half). Accordingly, 7,061 genes are over-expressed in the tentacular system (sample B2) compared to the control sample (B1). With application of this filter, 5,664 genes belonged to one of the eight differential expression profiles defined above for experiment A.

## *2.2 Validation of the RNAseq data by confrontation with ISH expression patterns*

As a first validation step, we performed ISH in the tentacular system for 28 genes (Fig. 3A) randomly selected to represent 7 of the expression profiles defined above for experiment A (Fig. 2): for each expression profile, four genes were taken from the list of most highly differentially expressed genes. Expression profile Ext[1>2<3] was not considered here because it is only marginally represented in the unfiltered dataset and almost disappears in the filtered dataset, indicating that it corresponds to genes with high expression in the umbrella and tentacle and low expression in the bulb, thus irrelevant with respect to cellular dynamics within the tentacle bulb. The obtained ISH expression patterns (Fig. 3A) are largely consistent

with expectations from expression profile assignments derived from RNAseq data. For instance, the 4 genes representing the Prox[1>2,3] expression profile display strong ISH signal in the proximal extremity of the tentacle bulb only; whereas Prox[1>2>3] genes show gradually decreasing signal intensity from the base to the tip of the bulb, and Prox[1,2>3] genes show more uniformly high ISH signal along the bulb, except towards distal tip. As expected, genes with strong ISH staining in the tentacle all belong to the three "Dist" expression profiles (see for instance *Ckm*, *Atp23*, *Eng* and *Pkhd111* in Fig. 3A). Genes assigned to the Mid[1<2>3] expression profile are either strongly expressed throughout the bulb but not in the umbrella and in the tentacle, which is consistent with read count being higher for sample A2 than A1 and A3 (see *metalloendopeptidase* and *Coll3a1* in Fig. 3A); or they show distinctly more intense staining within the distal half of the tentacle bulb (see *FoxC1* and *c91059\_g4* in Fig. 3A).

Cases of apparent discrepancy between RNAseq-derived expression levels and ISH expression patterns systematically correspond to ISH signal intensity in the tentacle much lower than expected from the read counts. This is particularly spectacular for instance for *Pnpla8*, *c81194\_g1*, *c73146\_g1*, and *Mfsd* (Fig. 3A). This observation is in line with our experience with whole mount ISH in *C. hemisphaerica* medusae. Usually, staining of tentacle cells is more difficult to obtain than staining of bulb cells and requires longer colour development time. Among the 12 genes representing "Dist" expression profiles in Fig. 3A, some provided intense signal in the tentacle rather easily and quickly (e.g. *Eng*, *Pkhd111*, *Tonsl*), whereas for others, despite RNAseq indicating high expression in sample A3, the tentacle remained uncoloured even after long development time (with tentacle bulb meanwhile turning a very dark purple/black). We have no obvious explanation for this heterogeneity, which may possibly reflect probe-dependent effects, and/or differential properties of the tentacular cell types in which these genes are expressed.

We then compared RNAseq estimates of expression levels with ISH expression patterns for Wnt signalling genes (ligands and receptors) (Fig. 3B). We chose to focus on Wnt pathway components for two reasons: (1) normalised expression levels as calculated from RNAseq data (experiment A, unfiltered) indicate that most of them are differentially expressed along the proximo-distal axis and fall into one of the defined expression profiles; (2) Wnt signalling pathways likely play a major role in the *Clytia* tentacular system as they have been shown to regulate cell differentiation and axis formation/maintenance in several cnidarians. At this

point, we examine the distribution of Wnt signalling gene expression patterns exclusively along the proximo-distal axis of the tentacular system (for instances of polarised expression along the oral-aboral axis, see section 2.5.).

Most of Wnt ligand and receptor genes happen to belong to one of the expression profiles defined in Fig. 2, and all of these expression profiles except Ext[1>2<3] comprise at least one Wnt or Fz gene (Fig. 3B). For Wnt1b, Wnt5b, Wnt7 (Prox[1>2, 3]), Wnt11b and FzdIII (Prox[1>2>3]), the ISH staining is restricted to the proximal half of the tentacle bulb. The Wnt4 gene, according to ISH, is expressed in the tentacle bulb where its expression domain extends into the distal half, consistent with its RNAseq expression profile (Prox[1,2>3]). Conversely, high expression in the tentacle and distal part of the bulb, but not in the rest of the bulb, is observed by ISH for Wnt5 (Dist[1<2<3]), Wnt6 and Wnt8 (Dist[1<2, 3]). Finally, ISH for WntA reveals confined expression in an endodermal spot localised within the distal half of the tentacle bulb, in agreement with the Mid[1<2>3] expression profile of this gene from RNAseq data. The only Wnt gene for which there is a real mismatch between both expression data types is FzdIV. By ISH, we detected transcripts of this gene only in the proximal half of the bulb (in basi-epithelial ectodermal cells, Fig. 3B, lower row), whereas according to RNAseq, FzdIV should be about twice more highly expressed in the distal vs. proximal bulb half, and again twice more highly expressed in the tentacle. The inherent difficulties of obtaining ISH staining in the tentacle discussed above may partly explain this discrepancy.

The elaborated differential deployment of Wnt signalling components along the proximo-distal axis of the tentacular system suggests that the Wnt/ $\beta$ -catenin pathway and/or non-canonical Wnt pathways (such as Ca<sup>2+</sup> or PCP) could be involved in regulating progression along the nematoblast cellular lineage. In bilaterians, the Wnt/ $\beta$ -catenin pathway controls the balance between pluripotency/proliferation and differentiation in a wide variety of cellular lineages (Sokol, 2011; Kühl and Kühl, 2013; Visweswaran et al., 2015; Masuda and Ishitani, 2017). Experimental evidence suggests that this is also the case in cnidarians, with Wnt signalling apparently promoting either stem cell maintenance, cell fate determination or cell differentiation depending on the species and/or cellular contexts (Hemrich et al., 2012; Teo et al., 2006; Plickert et al., 2012; Guder et al., 2006b; Khalturin et al., 2007).

Finally, as a last validation step, we looked at expression values deduced from RNAseq (experiment A) for various published genes with clear proximo-distal polarity in the tentacle bulb according to the *in situ* hybridisation data available in the literature (Fig. 4D). In agreement with the published ISH patterns, for stem cell genes, such as *Vasa*, *Nanos1*, *Piwi*, *Sox10* (Denker et al. 2008, Leclère et al. 2012, Jager et al. 2011), RNAseq read counts are highest in the proximal part of the bulb (sample A1). The cell cycle regulators *CyclinB* and *CyclinD* (Coste et al. 2016) and the transcription factors *Sox11* and *Sox13* were strongly expressed in the bulb (A1 and A2) and much less in the tentacle. Nematocyst capsule genes, such as *Minicollagen*, *Nowa* (Denker et al. 2008) and *Nematogalectin* (Hwang et al. 2010) were highest in the distal part of bulb (A2) (see Fig. 4D for more genes and Tab. S1 for more details).

### 2.3. The expression profiles of stem-cell genes and nematocyst genes are consistent with the cellular conveyor belt model

To check whether the differential gene expression data of experiment A were consistent with the model of the cellular conveyor belt (i.e. ordered progression of the nematocyte cellular lineage along the proximo-distal axis of the tentacular system), we examined the expression profiles of two particular sets of genes: stem-cell genes, and genes associated with nematocyte differentiation. We compiled the list of *C. hemisphaerica* orthologues of the 227 genes of *Hydra magnipapillata* that according to the comparative analyses of Alié et al. (2015) belonged to the stem-cell gene toolkit of the last ancestor of Metazoa (hereafter, "stem-cell gene set" see Fig. 4A, Tab. S2). In the *C. hemisphaerica* tentacular system, according to previous studies (Denker et al., 2008; Coste et al., 2016), stem cells are restricted to the most proximal area of the bulb (close to its insertion point on the umbrella periphery), and proliferating progenitors of nematoblasts are present throughout the bulb except towards distal extremity. Similarly, we identified the orthologues in *C. hemisphaerica* of the 345 genes that in *Hydra* encode proteins of the nematocyte capsule (called nematocyst) (Balasubramanian et al., 2012) (hereafter, "nematocyst gene set" see Fig. 4B, Tab. S3). In the *C. hemisphaerica* tentacular system, we can roughly expect early markers of nematocyte differentiation to turn on in the proximal half of the bulb and later markers in the distal half. We checked that the relative frequencies of relevant Gene Ontology categories (e.g. DNA binding, DNA replication, peptidase activity, etc.) among these *C. hemisphaerica* "stem-cell" and

"nematocyte" sets or orthologues are in line with the content of these gene sets as described in the two source papers (Alié et al. 2015, Balasubramanian et al., 2012) (Fig. S1).

When compared to all genes, both gene sets (stem-cell and nematocyst) comprise a distinctly higher proportion of genes that are differentially expressed in experiment A (see numbers and percentage above bars in Fig. 5A-D). The magnitude of the difference is more spectacular in the unfiltered dataset (differentially expressed genes representing  $27,582/79,614 = 34.6\%$  of the total;  $118/169 = 69.8\%$  for the stem-cell gene set;  $104/119 = 87.4\%$  for the nematocyst gene set), because the filtered dataset overall comprises a much higher proportion of differentially expressed genes (total:  $5,664/7,061 = 80.2\%$ ; stem-cell:  $55/61 = 90.2\%$ ; nematocyte:  $94/99 = 94.9\%$ ).

The 55 genes that are differentially expressed among the filtered stem-cell gene set (Fig. 5C) comprise about 75% of Prox[1,2>3] (total genes: 51%, Fig. 5B) and 25% of Prox[1>2>3] (total genes: 5.4%). The high proportion of Prox[1>2>3] (genes whose expression decreases gradually from sample A1 to sample A3) is particularly significant, considering the stringency of the statistical criteria for a gene to be assigned to this expression profile (expression twice as high in sample A1 than in sample A2, *and* twice as high in sample A2 than in sample A3, with  $p_{adj} < 0.05$  for both comparisons). Expression profile Prox[1,2>3] corresponds to genes that have statistically significant higher expression in A1 and A2 with respect to A3 (but not A1 with respect to A2). Remarkably, among genes of the stem-cell set that belong to this profile, 93% have a higher read count for sample A1 than for sample A2 (not shown in Fig. 5C). In conclusion, genes of the stem-cell set tend to be over-expressed in the proximal half of the tentacle bulb, with respect to more distal parts of the tentacular system, in line with expectations from the conveyor belt model.

In the nematocyst gene set, the Prox[1,2>3] expression profile is strongly over-represented with respect to total genes (compare Fig. 5D with Fig. 5B), as in the stem-cell gene set. However, when looking at read counts, 72% of the Prox[1,2>3] nematocyst genes have more reads for sample A2 than for sample A1 (not shown in Fig. 5D), the opposite of what we observed for stem-cell genes. Another striking difference is that genes whose expression decreases gradually from sample A1 to sample A3 (Prox[1>2>3]) are marginally represented by only 1.1% of the genes in the filtered nematocyst set. Moreover, the expression profile Mid[1<2>3] (genes over-expressed in sample A2 with respect to both A1 and A3) is

represented by 3% of the genes in the filtered nematocyst gene set (6.4% among total filtered genes), whereas it is absent in the stem-cell gene set. Overall, the vast majority of nematocyst genes are over-expressed in the tentacle bulb (with respect to the mature tentacle), particularly in the distal half, in agreement with the cellular conveyor belt model. Low expression levels in sample A3 furthermore indicate that most genes coding for structural components of the capsule are turned off once differentiation is achieved, as shown in *Nematostella* (Sunagar et al. 2018).

#### *2.4. Comparisons of gene content among expression profiles sheds light on cellular dynamics in a cnidarian cellular conveyor belt*

We compared the relative frequencies of the 8 expression profiles among 11 selected categories of gene ontologies (GO), representing fundamental biological processes, molecular functions, and cell components (see M&M for more details on GO selection). The data are presented filtered in Fig. 5E-O and unfiltered in Fig. S2. Reciprocally, the proportions of these GO categories in each of the 8 expression profiles (and "others") are given in Fig. S3, S4. According to their behaviours in terms of differential expression along the tentacular system axis, these GO categories can be roughly classified in three groups: (i) GOs with mainly genes over-expressed in the proximal part of the tentacular system; (ii) GOs with approximately equal representation of genes with maximal expression in the proximal or distal parts of the tentacular system, (iii) GOs characterised by a dominance of genes with maximal expression in the distal part, i.e. tentacle (Fig. 5).

Not surprisingly, functional category "DNA replication" (Fig. 5G) belongs to the first group, with expression profiles Prox[1>2,3], Prox[1>2>3] and Prox[1,2>3] altogether representing 84% of the differentially expressed genes for this GO. This reflects restriction of cell proliferation to the tentacle bulb, consistent with experimental data (Denker et al., 2008; Coste et al., 2016), and with observations on the "stem-cell gene set". For GOs "DNA binding" (Fig. 5E) and "RNA binding" (Fig. 5F), the relative frequencies of expression profiles are similar, with a slightly higher proportion of the three 'Dist' profiles and Mid[1<2>3] for "DNA binding", and with no Prox[1>2,3] genes for "RNA binding".

Regarding functional categories "anatomical structure morphogenesis" (Fig. 5H) and "cytoskeleton" (Fig. 5J), there are approximately as many genes maximally expressed at the

proximal pole as at the distal pole of the cellular conveyor belt, and the frequencies of the 8 expression profiles are roughly similar to those observed for "all genes" (Fig. 5B). This may reflect strong functional heterogeneity of the genes associated with these GO categories, and/or that the corresponding biological processes and cellular components do not involve pronounced polarity of gene expression along the tentacular system axis.

GOs "neurological system process" (Fig. 5K), "synapse" (Fig. 5M) and "channel activity" (Fig. 5O) depart from "total genes" (Fig. 5B) by the much higher proportion of Dist[1<2<3] and Dist [1<2,3] expression profiles, in sharp contrast with previous observations concerning genes encoding nematocyst components. This suggests that a large part of the neuronal differentiation program is activated later than the nematocyte capsule construction program, in the distal part of the bulb. Further, neural genes are overall more transcriptionally active in the tentacle than are nematocyst genes. GO "channel activity" displays a percentage of genes with expression climbing stepwise from sample A1 to sample A3 (Dist[1<2<3]) much higher than for any of the other examined categories (48%). Among genes of this category are many genes annotated as glutamate, GABA, and acetylcholine receptors, as well as Ca<sup>2+</sup> channels.

In the case of GO "cell migration" (Fig. 5I), the relative proportions of the expression profiles are similar to those for all genes (Fig. 5B), but with a distinctly higher proportion of genes with expression increasing gradually from sample A1 to A3 (Dist[1<2<3]). The list of Dist[1<2<3] genes with a "cell migration" annotation (given in Tab. S4) comprises homologues of several proteins known in vertebrates for their role during neural development in cell body migration and/or axon guidance (slit, tenascin, neuropilin and girardin), several genes with high sequence similarity to angiopoietin (ligand of the TEK/TIE2 receptor, which in vertebrates is involved in endothelial cell proliferation, migration, adhesion and spreading during angiogenesis), and two fibrinogen-like sequences (precursor of the fibrin matrix, which notably acts during wound repair to stabilise the lesion and guide cell migration during re-epithelialisation). Even if active migration of nematocytes from their differentiation site to their final destination has not been demonstrated in medusae, these observations suggest that cell migration takes place in the *C. hemisphaerica* tentacular system, as is well documented in the *Hydra* polyp (Boehm and Bosch, 2012). In the polyp colony of *C. hemisphaerica*, nematogenesis is confined to the stolons, and nematocytes travel along polyp stems to join the polyp tentacles (unpublished observations).

Among surveyed functional categories, those with the highest enrichment in genes over-expressed in the tentacle (sample A3) are related to features of differentiated cells: "cilium" (Fig. 5N), "contractile fibre" (Fig. 5L), "neurological process" (Fig. 5K) and "channel activity" (Fig. 5O). This is consistent with the tentacle containing only differentiated cells. Among tentacle cell types, a cilium is present in nematocytes, sensory cells, and most ganglion cells. Category "cilium" displays a proportion of genes over-expressed in the tentacle (Dist[1,2<3]) higher than any other examined category, suggesting high transcriptional activity for maintenance of ciliary structures in differentiated cells of the tentacle.

The annotations of the genes showing the highest fold change ratios between samples in experiment A (Fig. 4C and Tab. S5) are consistent with our general views about the tentacular system and with analyses based on GO categories. Proteins acting in cell replication, such as mitotic proliferation cyclin kinase B, are represented in "Prox" profiles. Neuronal and muscular markers, such as glutamate receptor and microfibril-associated glyco 4 are found among the top genes of the three "Dist" profiles. The "top gene list" of Mid[1<2>3] profile genes contains many components of the extracellular matrix, notably collagens, in agreement with the hypothesis that the distal part of the bulb is the main place where cellular differentiation takes place. The most over-expressed genes in the Ext[1>2<3] profile are harder to categorise, which is not surprising given the special status of this expression profile.

### *2.5. Differential deployment of some Wnt signalling genes along the oral-aboral axis of the C. hemisphaerica tentacular system*

Closer examination of the expression patterns of Wnt signalling genes revealed that several of them are asymmetrically expressed along the oral-aboral axis of the tentacular system (Fig. 6), perpendicular to the proximo-distal axis discussed earlier (see Fig. 1B for a graphical representation of these two polarity axes). In order to clarify the gene expression patterns in 3D and along both polarity axes, whole-mount ISH of tentacular systems in Fig. 6 and 7 are shown in 3 orientations: frontal view (oral or aboral) (A, B, C, etc.); lateral view (A', B', C', etc.) and distal view (A'', B'', C'', etc.). The oral side is on the left for all lateral and distal views. Wnt signalling genes with oral-aboral polarised expression patterns are shown in Fig. 6 and those without apparent polarity along this axis are presented in Fig. 7.

Four Wnt ligand genes (Wnt3, Wnt4, Wnt7 and Wnt8) are expressed on the oral side only (Fig. 6A-D"), whereas one receptor (FzdII) and the antagonist Dkka are expressed on the aboral side only (Fig. 6E-F"). Wnt3 is expressed in the oral half of the tentacular system, all along bulb and tentacle (Fig. 6A-A"). Its expression domain border is rather sharply delimited. The expression domain of Wnt8 is more contracted along the midline on the oral side of the bulb and tentacle (Fig. 6D-D"). Wnt4 and Wnt7 are not expressed in the tentacle (Fig. 3B). Wnt4 has a wide triangular expression domain on the oral side of the tentacle bulb, in continuity with the nerve ring(s) in which it is also expressed (Fig. 6B-B"), whereas Wnt7 expression appears restricted to the nerve ring(s) (Fig. 6C-C"). The receptor FzdII (Fig. 6E-E") and the antagonist Dkka (Fig. 6F-F") are expressed along the aboral bulb midline (for FzdII, with lateral extensions of the expression domain along the bulb base, Fig. 6E) and along the tentacle in the form of a narrow aboral stripe (as visible in lateral views, Fig. 6E' and F').

Since Wnt3 has been functionally characterised in the polyp of hydra and the embryo of *C. hemisphaerica* as an oral activator of the Wnt/ $\beta$ -catenin pathway (Lengfeld et al. 2009, Momose et al. 2008), its expression, restricted to the oral half of the bulb and tentacle, together with the aboral expression domain of the antagonist Dkka, suggest differential activation of the Wnt/ $\beta$ -catenin pathway along the oral-aboral axis of the tentacular system, with a maximum of activity on the oral side. A role of the canonical Wnt pathway in establishment and maintenance of the oral-aboral (primary) body axis, with a Wnt secreting centre located at the oral pole, has been observed in all cnidarian species that have been investigated, from early embryonic stages (*C. hemisphaerica*, Momose and Houliston, 2007; Momose et al., 2008) to planulae (*C. hemisphaerica*; *Hydractinia echinata*, Plickert et al. 2006; Hensel et al. 2014 *Nematostella vectensis*, Marlow et al., 2013) and polyps (*Hydra*, Hobmayer et al., 2000; Bode, 2012; Gee et al., 2010; *Hydractinia echinata*, Plickert et al., 2006; Duffy et al., 2010; Hensel et al. 2014). This also likely holds true for medusae given localised expression of Wnt3 around the manubrium extremity (medusa bud of *Podocoryna carnea*: Sanders and Cartwright, 2015; medusa bud and medusa of *C. hemisphaerica*: our unpublished data).

In the local context of the medusa tentacular system of *C. hemisphaerica*, our results suggest that Wnt/ $\beta$ -catenin signalling has retained this function, meaning that it is deployed along an

axis (oral-aboral) that is perpendicular to the tentacular system elongation axis (the proximo-distal axis), and therefore perpendicular to the direction of progression along the cellular conveyor belt. In the *C. hemisphaerica* oocyte and embryo, Wnt3 activates the Wnt/ $\beta$ -catenin pathway through binding to FzdI, co-expressed at the oral pole (Momose and Houliston, 2007; Momose et al., 2008), whereas the aborally-expressed FzdIII receptor opposes FzdI function. The regulatory logic may be different in the context of the medusa tentacular system, where FzdI expression is ubiquitous (Fig. 7H-H"), FzdIII is expressed only towards the bulb base without any oral-aboral polarity (Fig. 7I-I"), and among the four Fz genes, only FzdII exhibits polarised expression along the oral-aboral axis but on the opposite side with respect to Wnt3. However, in *Nematostella vectensis*, FzdII has been shown to activate Wnt/ $\beta$ -catenin signalling at the oral pole despite being expressed at the aboral pole (Leclère et al., 2016). Therefore, a polarising function for a signal protein or receptor does not necessarily mimic the spatial distribution of its transcription sites. This also means that among Wnt signalling genes exhibiting no oral-aboral polarity of expression in the tentacular system (i.e., the 10 genes of Fig. 7), some may nevertheless be functionally involved in polarising this axis.

Previous studies addressing nematogenesis in the hydrozoan medusa tentacle bulb system have focused exclusively on how this process behaves with respect to the proximo-distal axis (the cellular conveyor belt model, depicted in Fig. 1A, Denker et al. 2008, Jager et al. 2011, Leclère et al. 2012, Coste et al. 2016). However, the oral-aboral axis of the tentacle bulb too has strong bearing on nematogenesis, because production of nematocytes occurs throughout the bulb ectoderm except along its aboral midline (Denker et al., 2008). Therefore, as a hypothesis to be tested in future experimental studies, differential activation of Wnt/ $\beta$ -catenin signalling on the oral side may promote the nematoblast fate. Reciprocally, the Wnt antagonist Dkka and the receptor FzdII may mediate inhibition of nematogenesis on the aboral side of the tentacle bulb.

The remarkable diversity of expression patterns exhibited by Wnt signalling genes in the tentacular system (Fig. 6 and 7) suggests that they play multiple and diverse roles beyond regulation of polarity axes and nematogenesis. This may notably include neural functions, as several genes are expressed in nerve ring(s) at the umbrella periphery (Wnt3, Fig. 6A; Wnt4, Fig. 6B, B'; Wnt6, Fig. 7E; Wnt7, Fig. 6C; FzdIII, Fig. 7I), and functions associated with the

endodermal component of the bulb and tentacle (see expression patterns of Wnt1b, Fig. 7A-A"; Wnt5b, Fig. 7D-D"; and WntA, Fig. 7G-G").

### 3. Conclusions

Our RNAseq-based expression analyses of samples staggered along the proximo-distal axis of the *C. hemisphaerica* medusa tentacular system revealed massive differential gene expression and brought strong additional support in favour of the cellular conveyor belt model (i.e. ordered progression of nematogenesis along the proximo-distal axis). These transcriptomic analyses also provided interesting cues revealing differential timings of transcription, along this conveyor belt, and of gene functional groups associated with different cellular components (e.g. nematocyte capsule vs. neuronal proteins vs. cilia). Furthermore, our detailed expression analyses of Wnt signalling genes draws attention to the fact that the cellular conveyor belt model does not fully account for the complexity of the tentacle bulb. Most Wnt and Fzd genes are differentially expressed along the proximo-distal axis, but some are instead (or also) differentially expressed along the oral-aboral axis. Bilaterality is defined by the existence of two perpendicular polarity axes (Manuel 2009). Our results suggest that the differential spatial deployment, along both polarity axes, of the diverse members of a single family of ligands (and corresponding receptors) contribute to the bilateral symmetry of a cnidarian organ.

We hope that the transcriptomic data generated in this study will stimulate and facilitate future research on cellular and molecular mechanisms operating in the tentacular system of the *C. hemisphaerica* medusa, including functional studies of Wnt signalling and other pathways in order to better understand their role with respect to polarities and tissue homeostasis.

## 4. Materials and Methods

### 4.1. Preparation of samples for RNAseq

All *C. hemisphaerica* medusae used for sample preparation were female genetic clones produced by the same polyp colony (Z4B strain, originally produced by in-breeding offspring from wild individuals in the E. Houliston's lab in Villefranche-sur-Mer). They were grown up in the lab in artificial seawater until the 16-tentacle stage. Micro-dissections of medusae were performed under a Leica MZ16 stereomicroscope, in 0.22  $\mu\text{m}$  filtered artificial seawater in Petri dishes coated with a 5 mm bottom layer of agarose 1.7% (previously dissolved in filtered artificial seawater). Medusae were maintained attached to the agarose bottom, with the subumbrellar side below and in flat configuration. For experiment A, medusae were immobilised using a device made of an entomological pin bearing a disk of rigid transparent plastic film (of diameter about half that of the medusa). The pin was stuck into the agarose through the centre of the medusa, and a controlled pressure was exerted on the umbrella by the plastic disk, until the umbrella adopted a flat shape with all tentacle bulbs accessible on the periphery. For experiment B, medusae were simply attached to the agarose bottom using 4 micro-pins. All cuts were done using surgical micro-scissors (Euronexia ultra-thin scissors, blade 3 mm long).

Samples A1, A2 and A3 (as illustrated in top left part of Fig. 1A) were prepared in the following order. First, the tentacle was gently stretched using forceps in order to extend the bulb, which was then cut at midlength between its base and the tentacle insertion point. The tentacle was then sectioned slightly above its insertion point on the bulb, which produced samples A2 and A3. Then the proximal half the bulb was separated from the medusa periphery by cutting into the umbrella around bulb base, providing sample A1. Samples prepared from the same medusa were stored separately in three rectangular holes bored into the agarose bottom, until all 16 tentacle bulbs of the medusa were dissected (about 30 min). At the end, the agarose was sculptured around each hole to form an agarose "spoon" which was used for transfer of samples into a 1.5 ml tube. This transferring technique was adopted because tentacles and tentacle bulbs are extremely sticky, preventing the use of forceps or a pipette. Two biological replicates were prepared for each sample (A1 to A3). A total of 82 tentacular systems were used per replicate.

In experiment B, sample B1 (bottom left part of Fig. 1A) consisted of medusae deprived of all regions that according to the marker gene survey of Denker et al. (2008) undergo nematogenesis and/or comprise concentration of stem cells, i.e. the tentacle bulbs, the manubrium, and the four gonads (with associated portions of radial canals). The removed tentacle bulbs and tentacles (latter shortened to a length equalling about 3 times that of the bulb), together with a small piece of peripheral umbrella and velum, formed sample B2. Two biological replicates were prepared for each sample (B1 from 5 medusae per replicate; B2 from 87 tentacular systems per replicate).

The presence in samples A1 and B2 of a piece of peripheral umbrella around the tentacle bulb base was the result of a deliberate choice given that in practice, it is impossible to cut exactly along the limit between tentacle bulb and umbrella. Therefore, to avoid removing part of the bulb base from these samples, it was necessary to cut within the umbrella at some distance from the bulb. Transcripts of genes expressed in this small part of peripheral umbrella are expected to be present at much higher levels in sample B1 than in sample B2, allowing for their subsequent subtraction, notably for data analyses of experiment A. It can furthermore be noticed from the procedure described above and from Fig. 1A, that sample A2 contains a short portion of tentacle (equivalent to about half the length of the bulb) in addition to the distal half of the tentacle bulb. This was done for two reasons: (i) to prevent any risk of removal of the distal bulb tip during the cut; (ii) because within the duration of sample preparation, it would have been impossible in practice to obtain distal bulb halves without any piece of tentacle. Indeed, after tentacle removal, regeneration at the distal extremity of the bulb starts immediately and proceeds very quickly, so that within just a few minutes, a short portion of newly formed tentacle becomes visible.

After transfer in 1.5 ml tubes in seawater, samples were centrifuged at 1,500 g for 2 min. Then the volume of seawater was reduced to about 50  $\mu$ l before addition of 300  $\mu$ l of lysis buffer (Ambion, RNAqueous<sup>®</sup> MicroKit), vortexing, and immediate freezing in liquid nitrogen. Samples were stored at -80°C until RNA preparation.

#### *4.2. RNA preparation and sequencing*

Total RNA was prepared from each sample using the RNAqueous<sup>®</sup> MicroKit (Ambion) according to instructions from the manufacturer. They were treated with DNase I (TURBO

DNase Kit, Ambion) for 20 min at 37°C (2 units per sample) then purified using the RNeasy minElute Cleanup kit (Quiagen). Quantities of total RNA (evaluated with nanodrop) were as follows: experiment A (first biological replicate / second biological replicate): sample A1 (390 ng / 380 ng), sample A2 (277 ng / 292 ng), sample A3 (203 ng / 230 ng); experiment B: sample B1 (780 ng / 847 ng), sample B2 (1.2 µg / 2.8 µg). Total RNA quality checks were performed using the Agilent 2100 Bioanalyzer.

Purification of mRNA and construction of a non-directional cDNA library were performed at the Genomic Paris Centre platform (IBENS, Paris) using the Illumina TruSeq RNA kit. Each biological replicate of experiment B was subdivided into two technical replicates (this was not done for experiment A due to more limiting RNA quantities). Sequencing using the Illumina technology (single reads 50 cycles, > 20M reads per sample) was performed at Genomic Paris Centre on a HiSeq 1500 sequencing system. The illumina raw data was deposited at the European Nucleotide Archive – accession number: PRJEB32346.

#### 4.3. Reference transcriptome

The reference transcriptome contains 161,887 transcripts assembled from Illumina cDNA sequencing of distinct stages of the life cycle of *Clytia hemisphaerica* (planula, polyp colony, baby and mature jellyfish, oocytes, accession number: PRJEB32564; see Leclère et al 2019 for more details).

#### 4.4. Differential gene expression analyses

Differential gene expression (DGE) analyses followed the same general workflow for both experiments (special points of divergence mentioned when needed). Reads from each biological duplicate were mapped to reference transcripts using kallisto, with 100 bootstraps. Since the data consisted of single-end reads, after several tries comparing the quality of the mapping for different parameter choices, we set the “estimated average fragment length” to 210 and the “estimated standard deviation of fragment length” to 10. The resulting abundance files were imported and compiled through tximport and tximportData packages in R, to obtain a count matrix. Then gene expression levels (expressed in read counts) were normalised (see Anders and Hubers, 2010) and calculated using the DESeq2 package in R. For experiment B, both technical replicates of each biological replicate were summed up before this step. The

table of correspondence between transcript isoforms resulting from Cufflinks was used to sum up expression levels at the scale of the genes. Using DESeq2 we performed pairwise comparisons for all conditions, after which (using standard filtering parameters in DESeq2) outliers as well as genes with low normalised mean counts were discarded. After this filtering step, 79,614 genes remained (Tab. S6). The resulting tables were gathered into a master comparison file for each condition. Duplicate reproducibility was checked by principal component analysis, heat map, and MA-plots, through the DESeq2 package (see Fig. S5).

In order to reduce computational time the annotation process was carried out only using Blast2GO and on a limited number of selected species (*Arabidopsis thaliana*, *Saccharomyces cerevisiae*, *Caenorhabditis elegans*, *Drosophila melanogaster*, *Danio rerio*, *Homo sapiens*, *Mus musculus*, *Rattus norvegicus*, *Nematostella vectensis*, *Thelohanellus kitauei*, *Hydra vulgaris*). The annotated gene list in this study is thus likely an underestimate of what it would be under a multi-pronged approach. Mapping, annotation, annotation augmentation and gene ontology (GO) propagation were performed using standard parameters in the software. Analyses of the relative frequencies of expression profiles across various gene lists (e.g. genes corresponding to a given GO; “stem-cell” and “nematocyst” genes, see below) were done through R. GO categories were selected from the complete GO list for those relevant to the bulb system (e.g. cellular dynamics, represented cell types).

#### 4.5. *Compilation of nematocyst and stem-cell gene sets*

The nematocyst gene set corresponds to the 119 genes in *Clytia* which returned a reciprocal first tBlast-n hit with the 345 genes coding for the total nematocyst proteome of *Hydra magnipapillata*, (435 genes) after exclusion of contaminants (25 genes) and genes also expressed in HU-treated nematocyst-free hydras (65 genes) (Balasubramanian et al., 2012). The list of stem-cell genes corresponds to the 169 genes in *Clytia* which returned a reciprocal first hit with the 227 genes of *H. magnipapillata* identified as belonging to the stem-cell gene toolkit of the last ancestor of Metazoa, by Alié et al. (2015).

#### 4.6. *“Top list” of representative genes from each expression profile*

The list of genes belonging to each expression profile was ordered by fold change, and the top annotated genes (when possible) were compiled into Tab. 5.

#### 4.7 GO selection

As a first step, we browsed all first and second level GO terms for "biological processes" "molecular functions", and "cell components" and retained the terms that seemed most relevant with respect to what we know about the jellyfish tentacular system (in terms of cell types and cellular dynamics). Then we eliminated redundancy between these pre-selected terms and also removed the terms to which a very low number of genes were assigned in our dataset, to obtain the final selection of 11 GO terms.

#### 4.8 ISH validation of the RNAseq results

Four genes were selected among the most differentially expressed genes ("top gene list") of each expression profile according to the following criteria applied in this order: (i) presence of sequence(s) of the gene in the Sanger EST collection of Chevalier et al. (2006), because physical clones of these ESTs are available in our lab, making probe synthesis easier; (ii) existence of an annotation for the gene; (iii) fold change values. For some of the expression profiles, the "top gene list" did not contain 4 genes that were at the same time present in the EST collection and with an annotation, in which case the first criterion was favoured.

Medusae were left unfed during 24 h before fixation. They were fixed during 40 min at 4°C in 3.7% formaldehyde, 0.2% glutaraldehyde in PBT (10 mM Na<sub>2</sub>HPO<sub>4</sub>, 150 mM NaCl, pH 7.5, 0.1% Tween 20). After fixation, specimens were washed three times in PBT and dehydrated through a graded series of ethanol, and stored in methanol at -20°C. The reciprocal procedure was used for rehydration before *in situ* hybridisation. Two different protocols were used for *in situ* hybridisation, using for the hybridisation step either formamide (as described in Jager et al., 2011) or urea (as described in Sinigaglia et al., 2018). Both protocols were used for all genes and the results were cross-checked for reproducibility.

#### 4.9 Molecular phylogeny of Wnt

Fzd genes were classified according to Schenkelaars et al., 2015. The sequences of Wnt genes available for two species of anthozoans (*Acropora palmata* and *Nematostella vectensis*), two species of hydrozoans (*C. hemisphaerica* and *H. vulgaris*), and one species of scyphozoans (*Aurelia aurita*) were gathered (Leclère et al. 2019, Khalturin et al. 2019). Amino-acid

sequences were aligned with ClustalOmega (Sievers et al., 2011) using standard parameters. The ambiguously-aligned parts of the alignment were removed thanks to an R script (R Core Team, 2017), based on the number of sequences and the similarity score at a given position. Preceding and following this step, the alignment was manually checked and curated for minor alignment errors using BioEdit (Hall, 1999). The final alignment used for the analysis comprises 330 sites, including 328 parsimony-informative positions, for 61 genes. Phylogenetic analysis was performed using the Maximum Likelihood method in RAxML (Stamatakis, 2014), with the LG (Le and Gascuel, 2008) +  $\Gamma$ 4 + I model. The tree was not rooted due to LBA (Long Branch Attraction) artefacts that are suspected to strongly perturbate its topology (compare Kusserow et al., 2005 and Hensel et al., 2014). Phylogenetic analyses supporting orthologies of *C. hemisphaerica* Wnt genes with those of *Nematostella vectensis* in Fig. S6; correspondence with names given in previous studies when different are given in Fig. S7;

## **Acknowledgements**

We thank Philippe Dru (UMR7009, Villefranche-sur-Mer) for performing the assembly of the *C. hemisphaerica* reference transcriptome. This work was supported by grants from the ‘‘Agence Nationale de la Recherche’’ ANR-09-BLAN-0236 DiploDevo and ANR-13-PDOC-0016 MEDUSEVO and from the Institut Universitaire de France (IUF). The École Normale Supérieure genomic core facility was supported by the France Génomique national infrastructure, funded as part of the "Investissements d'Avenir" program managed by the Agence Nationale de la Recherche (contract ANR-10-INBS-09). The funders had no role in study design, data collection and analysis, decision to publish, or preparation of the manuscript.

## **Competing interests**

The authors declare that there is no financial or other potential conflict of interests.

## References

- Alié, A., Leclère, L., Jager, M., Dayraud, C., Chang, P., Le Guyader, H., Quéinnec, E., Manuel, M., 2011. Somatic stem cells express Piwi and Vasa genes in an adult ctenophore: ancient association of « germline genes » with stemness. *Dev. Biol.* 350, 183-197.
- Alié, A., Hayashi, T., Sugimura, I., Manuel, M., Sugano, W., Mano, A., Satoh, N., Agata, K., Funayama, N., 2015. The ancestral gene repertoire of animal stem cells. *Proc. Natl. Acad. Sci. USA* 112(51), E7093-7100.
- Anders, S., Huber, W., 2010. Differential expression analysis for sequence count data. *Genome Biol.* 11(10), R106.
- Balasubramanian, P.G., Beckmann, A., Warnken, U., Schnölzer, M., Schüler, A., Bornberg-Bauer, E., Holstein, T.W., Ozbek, S., 2012. Proteome of Hydra nematocyst. *J. Biol. Chem.* 287(13), 9672-9681.
- Bielen, H., Houart, C., 2014. The Wnt cries many: Wnt regulation of neurogenesis through tissue patterning, proliferation, and asymmetric cell division. *Dev. Neurobiol.* 74(8), 772-780.
- Bode, H.R., 1996. The interstitial cell lineage of hydra: a stem cell system that arose early in evolution. *J. Cell Sci.* 109, 1155-1164.
- Bode, H.R., 2012. The head organizer in Hydra. *Int J Dev Biol* 56, 473-478.
- Boehm, A.M., Bosch, T.C.G., 2012. Migration of multipotent interstitial stem cells in hydra. *Zoology* 115, 275–282.
- Candal, E., Thermes, V., Joly, J.S., Bourrat, F., 2004. Medaka as a model system for the characterization of cell cycle regulators: a functional analysis of Ol-GADD45 during early embryogenesis. *Mech. Dev.* 131, 945–958.
- Candal, E., Alunni, A., Thermes, V., Jamen, F., Joly, J.S., Bourrat, F., 2007. Ol-Insm1b, a SNAG family transcription factor involved in cell cycle arrest during medaka development. *Dev. Biol.* 309, 1–17.
- Coste, A., Jager, M., Chambon J.-P., Manuel, M., 2016. Comparative study of Hippo pathway genes in cellular conveyor belts of a ctenophore and a cnidarian. *EvoDevo* 7, 4.
- Dayraud, C., Alié, A., Jager, M., Chang, P., Le Guyader, H., Manuel, M., Quéinnec, E., 2012. Independent specialisation of myosin II paralogues in muscle vs. non-muscle functions during early animal evolution: a ctenophore perspective. *BMC Evol. Biol.* 12, 107.
- Demilly, A., Steinmetz, P., Gazave, E., Marchand, L., Vervoort, M., 2013. Involvement of the Wnt/ $\beta$ -catenin pathway in neurectoderm architecture in *Platynereis dumerilii*. *Nat. Comm.* 4, 1915.
- Denker, E., Manuel, M., Leclère, L., Le Guyader, H., Rabet, N., 2008. Ordered progression of nematogenesis from stem cells through differentiation stages in the tentacle bulb of *Clytia hemisphaerica* (Hydrozoa, Cnidaria). *Dev. Biol.* 315, 99-113.
- Devès, M., Bourrat, F., 2012. Transcriptional mechanisms of developmental cell cycle arrest: problems and models. *Semin. Cell. Dev. Biol.* 23, 290–297.
- Duffy, D.J., Plickert, G., Kuenzel, T., Tilmann, W., Frank, U., 2010. Wnt signaling promotes oral but suppresses aboral structures in *Hydractinia* metamorphosis and regeneration. *Development* 137(18), 3057-3066.
- Garcin, C.L., Habib, S.J., 2017. A comparative perspective on Wnt/ $\beta$ -catenin signalling in cell fate determination. *Results Probl. Cell Differ.* 61, 323-350.
- Gee, L., Hartig, J., Law, L., Wittlieb, J., Khalturin, K., Bosch, T.C., Bode, H.R., 2010. Beta-catenin plays a central role in setting up the head organizer in hydra. *Dev. Biol.* 340, 116-124.

- Guder, C., Philipp, I., Lengfeld, T., Watanabe, H., Hobmayer, B., Holstein, T.W., 2006a. The Wnt code: cnidarians signal the way. *Oncogene* 25, 7450-7460.
- Guder, C., Pinho, S., Nacak, T.G., Schmidt, H.A., Hobmayer, B., Niehrs, C., Holstein, T.W., 2006b. An ancient Wnt-Dickkopf antagonism in Hydra. *Development* 133(5), 901-911.
- Hall, T.A., 1999. BioEdit: a user-friendly biological sequence alignment editor and analysis program for Windows 95/98/NT. *Nucleic Acids Symp. Ser.* 41, 95–98.
- Hemrich, G., Khalturin, K., Boehm, A.-M., Puchert, M., Anton-Erxleben, F., Wittlieb, J., Klostermeier, U.C., Rosenstiel, P., Oberg, H.H., Domazet-Lozo, T., Sugimoto, T., Niwa, H., Bosch, T.C., 2012. Molecular signatures of the three stem cell lineages in Hydra and the emergence of stem cell function at the base of multicellularity. *Mol. Biol. Evol.* 29, 3267-3280.
- Hensel, K., Lotan, T., Sanders, S.M., Cartwright, P., Frank, U., 2014. Lineage-specific evolution of cnidarian Wnt ligands. *Evol. Dev.* 16(5), 259-269.
- Hobmayer, B., Rentzsch, F., Kuhn, K., Happel, C.M., von Laue, C.C., Snyder, P., Rothbacher, U., Holstein, T.W., 2000. WNT signalling molecules act in axis formation in the diploblastic metazoan Hydra. *Nature* 407(6801), 186-189.
- Holló, G., 2017. Demystification of animal symmetry: symmetry is a response to mechanical forces. *Biol. Direct* 12(1), 11.
- Hwang, J.S., Takaku, Y., Momose, T., Adamczyk, P., Özbek, S., Ikeo, K., Khalturin, K., Hemrich, G., Bosch, T.C., Holstein, T.W., David, C.N., Gojobori, T., 2010. Nematogalectin, a nematocyst protein with GlyXY and galectin domains, demonstrates nematocyte-specific alternative splicing in Hydra. *Proc Natl Acad Sci U S A.* 107, 18539-18544.
- Jager, M., Quéinnec, E., Le Guyader, H., Manuel, M., 2011. Multiple *Sox* genes are expressed in stem cells or in differentiating neuro-sensory cells in the hydrozoan *Clytia hemisphaerica*. *EvoDevo* 2, 12.
- Jager, M., Dayraud, C., Mialot, A., Quéinnec, E., Le Guyader, H., Manuel, M., 2013. Evidence for involvement of Wnt signalling in body polarities, cell proliferation, and the neurosensory system in an adult ctenophore. *PLoS One* 8(12), e84363.
- Joly, J.S., Recher, G., Brombin, A., Ngo, K., Hartenstein, V., 2016. A conserved developmental mechanism builds complex visual systems in insects and vertebrates. *Curr. Biol.* 26(20), R1001-R1009.
- Khalturin, K., Anton-Erxleben, F., Milde, S., Plötz, C., Wittlieb, J., Hemrich, G., Bosch, T.C., 2007. Transgenic stem cells in Hydra reveal an early evolutionary origin for key elements controlling self-renewal and differentiation. *Dev. Biol.* 309: 32-44.
- Khalturin, K., Shinzato, M., Khalturina, et al. 2019. Medusozoan genomes inform the evolution of the jellyfish body plan. *Nat. Ecol. Evol.* 3:811-822.
- Kühl, S.J., Kühl, M., 2013. On the role of Wnt/ $\beta$ -catenin signaling in stem cells. *Biochim Biophys. Acta* 1830, 2297-2306.
- Lapébie, P., Gazave, E., Ereskovsky, A., Derelle, R., Bézac, C., Renard, E., Houlston, E., Borchiellini, C., 2009. WNT/beta-catenin signalling and epithelial patterning in the homoscleromorph sponge *Oscarella*. *PLoS One* 4(6), e5823.
- Lapébie, P., Borchiellini, C., Houlston, E., 2011. Dissecting the PCP pathway: one or more pathways? *Bioessays* 33, 759-768.
- Lapébie, P., Ruggiero, A., Barreau, C., Chevalier, S., Chang, P., Dru, P., Houlston, E., Momose, T., 2014. Differential responses to Wnt and PCP disruption predict expression and developmental function of conserved and novel genes in a cnidarian. *PLoS Genet.* 10(9), e1004590.
- Le, S.Q., and Gascuel, O., 2008. An improved general amino acid replacement matrix. *Mol. Biol. Evol.* 25, 1307–1320.

- Leclère, L., Jager, M., Barreau, C., Chang, P., Le Guyader, H., Manuel, M., Houliston, E. 2012., Maternally localized germ plasm mRNAs and germ cell/stem cell formation in the cnidarian *Clytia*. *Dev. Biol.* 364, 236-248.
- Leclère, L., Bause, M., Sinigaglia, C., Steger, J., Rentzsch, F., 2016. Development of the aboral domain in *Nematostella* requires b-catenin and the opposing activities of Six3/6 and Frizzled5/8. *Development* 143(10), 1766-1777.
- Leclère, L., Horin, C., Chevalier, S., Lapébie, P., Dru, P., Peron, S., Jager, M., Condamine, T., Pottin, K., Romano, S., Steger, J., Sinigaglia, C., Barreau, C., Quiroga Artigas, G., Ruggiero, A., Fourrage, C., Kraus, J.E.M., Poulain, J., Aury, J.M., Wincker, P., Quéinnec, E., Technau, U., Manuel, M., Momose, T., Houliston, E., Copley, R.R., 2019. The genome of the jellyfish *Clytia hemisphaerica* and the evolution of the cnidarian life-cycle. *Nat. Ecol. Evol.* doi: 10.1038/s41559-019-0833-2.
- Leininger, S., Adamski, M., Bergum, B., Guder, C., Liu, J., Laplante, M., Brâte, J., Hoffmann, F., Fortunato, S., Jordal, S., Rapp, H.T., Adamska, M., 2014. Developmental gene expression provides clues to relationships between sponge and eumetazoan body plans. *Nat. Comm.* 5, 3905.
- Lengfeld T1, Watanabe H, Simakov O, Lindgens D, Gee L, Law L, Schmidt HA, Ozbek S, Bode H, Holstein TW. 2009. Multiple Wnts are involved in Hydra organizer formation and regeneration. *Dev Biol.* 330(1):186-99.
- Loh, K.M., van Amerongen, R., Nusse, R., 2016. Generating cellular diversity and spatial form: wnt signaling and the evolution of multicellular animals. *Dev. Cell* 38(6), 643-655.
- Manuel, M., 2009. Early evolution of symmetry and polarity in metazoan body plans. *C. R. Biol.* 332, 184-209.
- Marlow, H., Matus, D.Q., Martindale, M.Q., 2013. Ectopic activation of the canonical wnt signalling pathway affects ectodermal patterning along the primary axis during larval development in the anthozoan *Nematostella vectensis*. *Dev. Biol.* 380, 324-334.
- Masuda, T., Ishitani, T., 2017. Context-dependent regulation of the  $\beta$ -catenin transcriptional complex supports diverse functions of Wnt/ $\beta$ -catenin signaling. *J. Biochem.* 161(1), 9-17.
- Momose T., Houliston, E., 2007. Two Oppositely Localised Frizzled RNAs as Axis Determinants in a Cnidarian Embryo. *PLoS Biol.* 5, e70.
- Momose, T., Derelle, R., Houliston, E., 2008. A maternally localised Wnt ligand required for axial patterning in the cnidarian *Clytia hemisphaerica*. *Development* 135, 2105-2113.
- Momose, T., Kraus, Y., Houliston, E., 2012. A conserved function for Strabismus in establishing planar cell polarity in the ciliated ectoderm during cnidarian larval development. *Development* 139(23), 4374-4382.
- Mulligan, K.A., Cheyette, B.N., 2012. Wnt signalling in vertebrate neural development and function. *J. Neuroimmune Pharmacol.* 7, 774-787.
- Niehrs, C., 2010. On growth and form: a Cartesian coordinate system of Wnt and BMP signalling specifies bilaterian body axes. *Development* 137, 845-857.
- Noelanders, R., Vleminckx, K., 2017. How Wnt signaling builds the brain: bridging development and disease. *Neuroscientist* 23(3), 314-329.
- Petersen, C.P., Reddien, P.W., 2009. Wnt signaling and the polarity of the primary body axis. *Cell* 139, 1056-1068.
- Plickert, G., Jacoby, V., Frank, U., Müller, W.A., Mokady, O., 2006. Wnt signaling in hydroid development: formation of the primary body axis in embryogenesis and its subsequent patterning. *Dev. Biol.* 298, 368-378.
- Plickert, G., Frank, U., Müller, W.A., 2012. *Hydractinia*, a pioneering model for stem cell biology and reprogramming somatic cells to pluripotency. *Int. J. Dev. Biol.* 56(6-8), 519-534.
- R Core Team, 2017. R: A Language and Environment for Statistical Computing.

- Ryan, J.F., Baxevanis, A.D., 2007. Hox, Wnt, and the evolution of the primary body axis: insights from the early-divergent phyla. *Biology Direct* 2, 37.
- Sanders, S.M., Cartwright, P., 2015. Patterns of Wnt signaling in the life cycle of *Podocoryna carnea* and its implications for medusae evolution in Hydrozoa (Cnidaria). *Evol. Dev.* 17(6), 325-336.
- Schenkelaars, Q., Fierro-Constain, L., Renard, E., Hill, A.L., Borchiellini, C., 2015. Insights into Frizzled evolution and new perspectives. *Evol. Dev.* 17(2), 160-169.
- Sievers, F., Wilm, A., Dineen, D., Gibson, T.J., Karplus, K., Li, W., Lopez, R., McWilliam, H., Remmert, M., Söding, J., et al., 2011. Fast, scalable generation of high-quality protein multiple sequence alignments using Clustal Omega. *Mol. Syst. Biol.* 7.
- Simion, P., Philippe, H., Baurain, D., Jager, M., Richter, D.J., Di Franco, A., Roure, B., Satoh, N., Quéinnec, E., Ereskovsky, A., Lapébie, P., Corre, E., Delsuc, F., King, N., Wörheide, G., Manuel, M., 2017. A large and consistent phylogenomic dataset supports sponges as the sister group to all other animals. *Curr. Biol.* 27, 958-967.
- Sinigaglia, C., Thiel, D., Hejnol, A., Houliston, E., Leclère L., 2018. A safer, urea-based in situ hybridization method improves detection of gene expression in diverse animal species. *Dev. Biol.* 434, 15-23.
- Steinmetz P.R., Kraus J.E., Larroux C., Hammel J.U., Amon-Hassenzahl A., Houliston E., Wörheide G., Nickel M., Degnan B.M., Technau U., 2012. Independent evolution of striated muscles in cnidarians and bilaterians. *Nature.* 487(7406), 231-234.
- Sokol, S.Y., 2011. Maintaining embryonic stem cell pluripotency with Wnt signaling. *Development* 138, 4341-4350.
- Sokol, S.Y., 2015. Spatial and temporal aspects of Wnt signaling and planar cell polarity during vertebrate embryonic development. *Semin. Cell Dev. Biol.* 42, 78-85.
- Stamatakis, A., 2014. RAxML version 8: A tool for phylogenetic analysis and post-analysis of large phylogenies. *Bioinformatics* 30, 1312–1313.
- Sunagar K, Columbus-Shenkar YY, Fridrich A, Gutkovich N, Aharoni R, Moran Y. 2018. Cell type-specific expression profiling unravels the development and evolution of stinging cells in sea anemone. *BMC Biol.* 16, 108.
- Teo, R., Möhrle, F., Plickert, G., Müller, W.A., Frank, U., 2006. An evolutionary conserved role of Wnt signaling in stem cell fate decision. *Dev. Biol.* 289, 91-99.
- Visweswaran, M., Pohl, S., Arfuso, F., Newsholme, P., Dilley, R., Pervaiz, S., Dharmarajan, A., 2015. Multi-lineage differentiation of mesenchymal cells – To Wnt, or not Wnt. *Int. J. Biochem. Cell Biol.* 68, 139-147.
- Zakharov, I.S., Hayes, N.L., Ierusalimski, V.N., Nowakowski, R.S., Balaban, P.M., 1998. Postembryonic neurogenesis in the procerbrum of the terrestrial snail, *Helix lucorum* L. *J. Neurobiol.* 35, 271–276.

## Figure legends

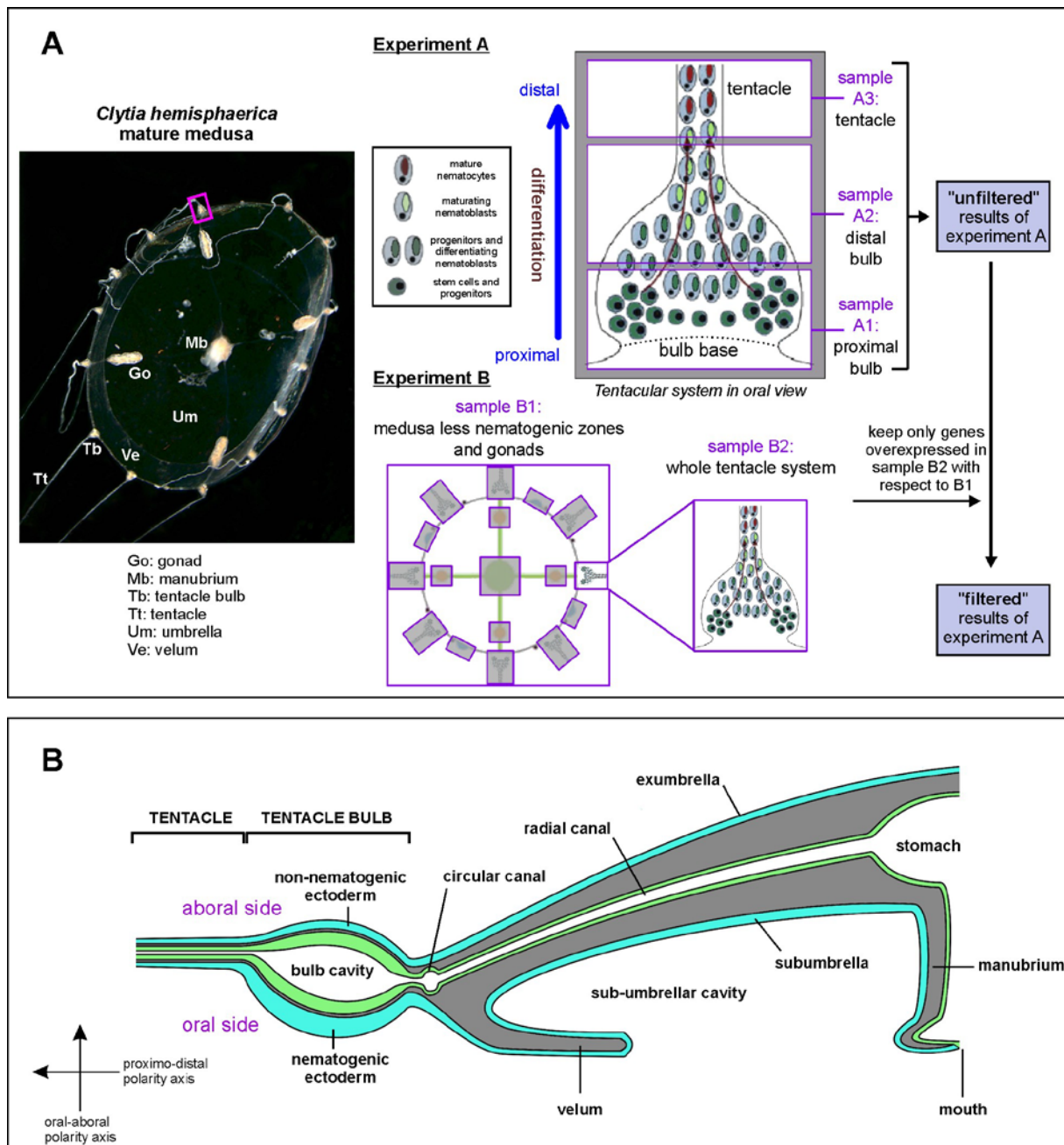


**Fig. 1.** The tentacular system in the medusa of *Clytia hemisphaerica*, with a summary of the experimental strategy used for differential gene expression analyses. (A) Spatial ordering of cellular stages along the proximo-distal axis of the tentacle bulb (cellular conveyor belt model), summary of sample preparation for experiments (B) The tentacular system in the context of oral-aboral polarity of the medusa anatomy. This scheme represents a section along one of the radial planes of the medusa. Blue: ectoderm; green: endoderm.

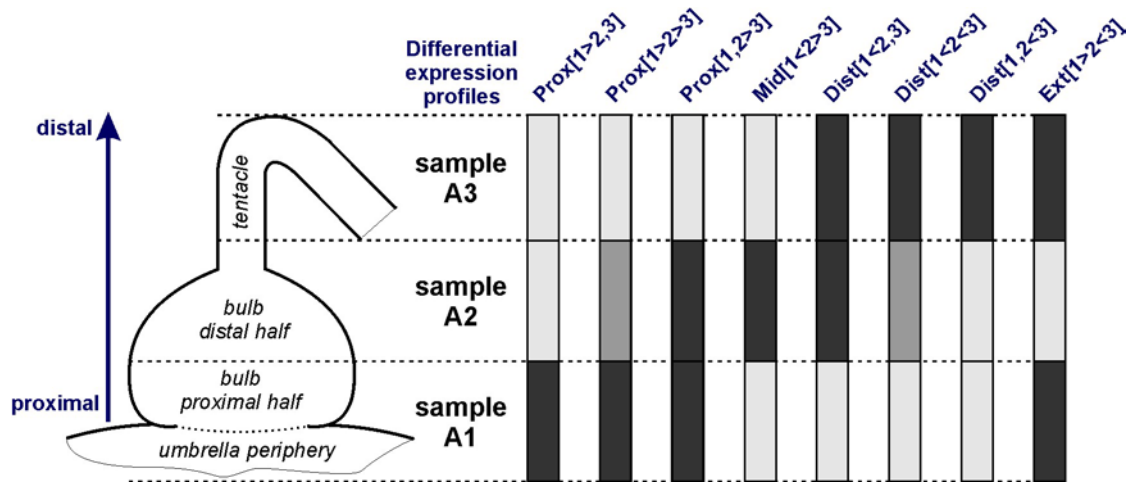


**Fig. 2.** Graphical definition of the 8 expression profiles. Darker grey color indicates higher relative expression.

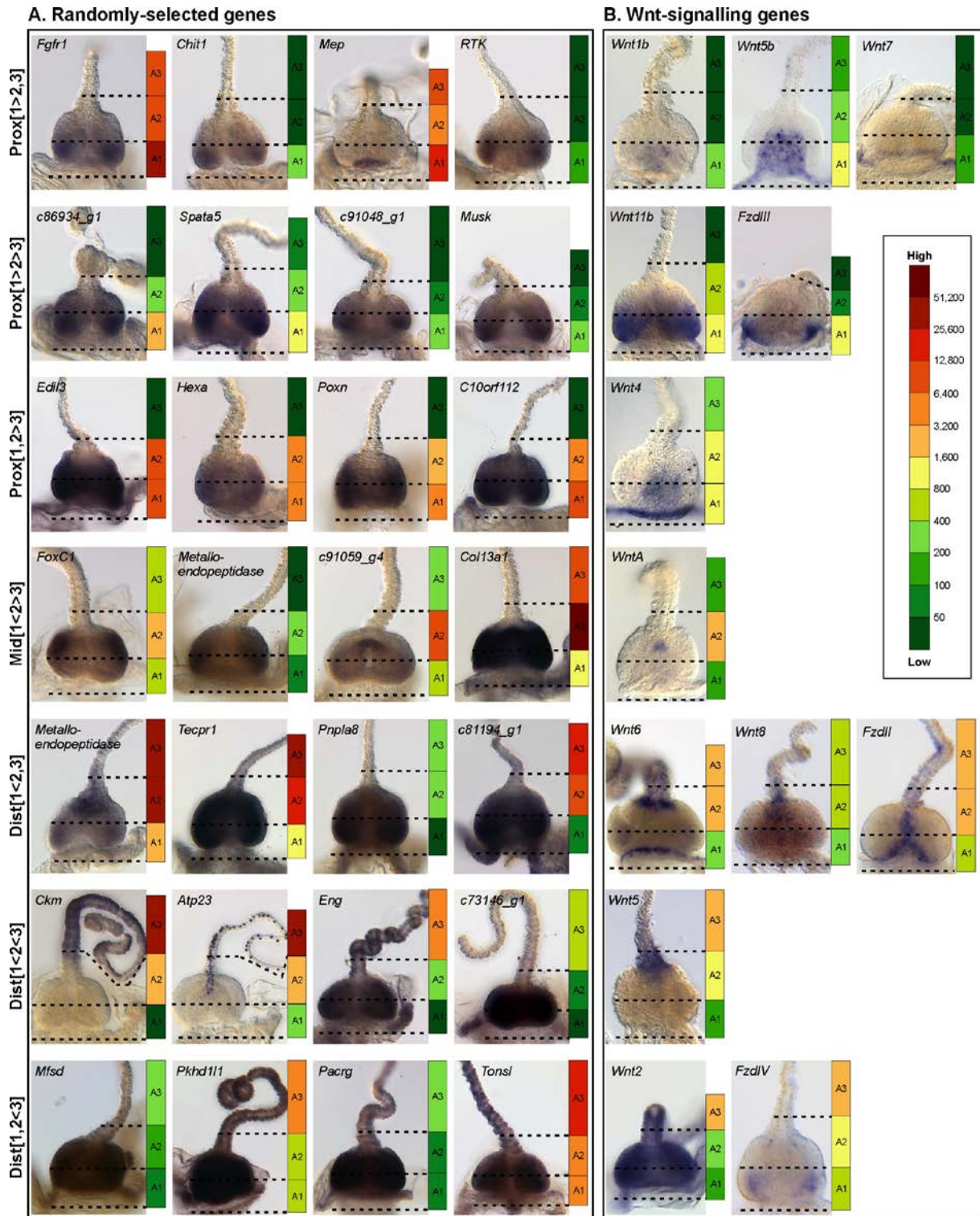


**Fig. 3.** ISH validation of the RNAseq results. (A) 4 randomly-selected genes per expression profile. (B) Wnt and Frizzled genes belonging to the expression profiles.



patterns that are differentially expressed in the experiment A. Expression values correspond to normalised read counts.

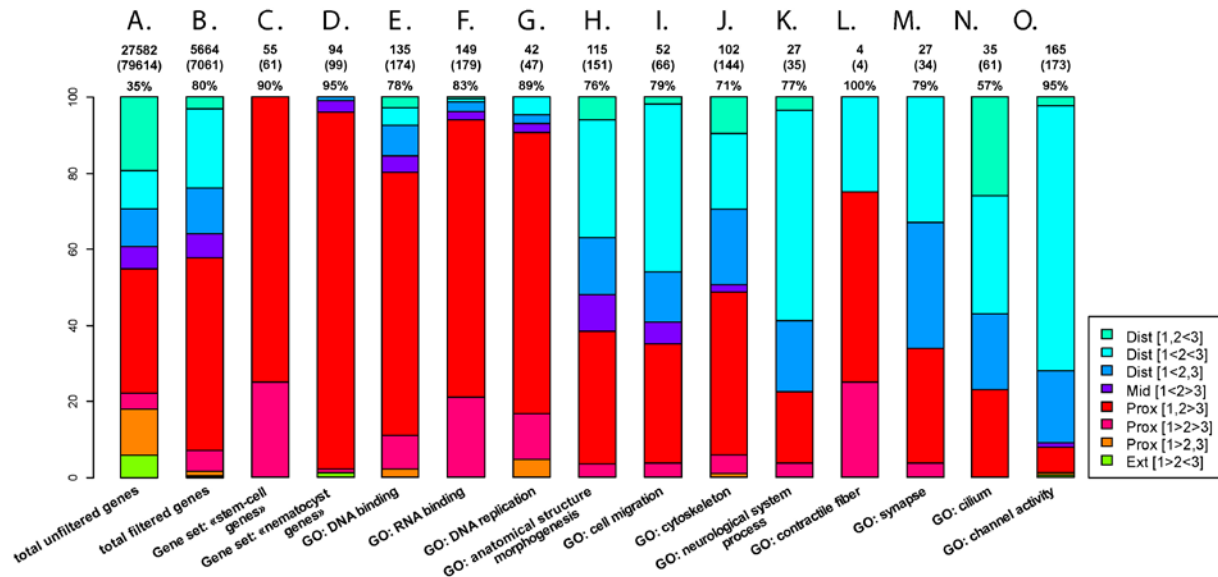
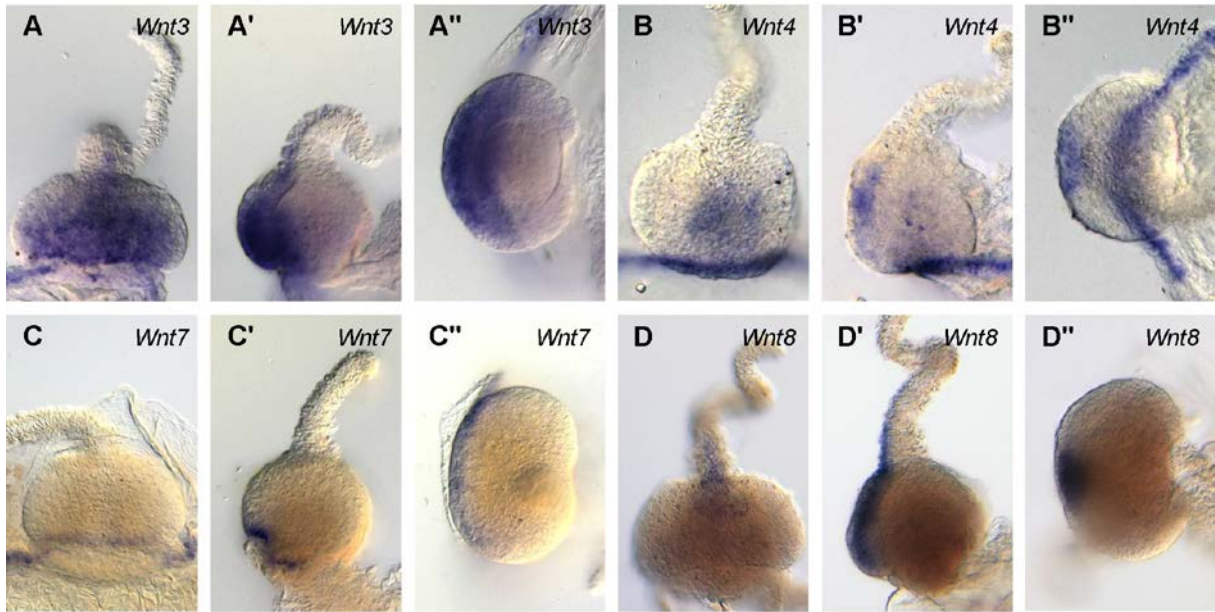


**Fig. 5.** Representation of the 8 expression profiles among the "total unfiltered genes"; "total unfiltered genes", "stem-cell genes" gene set, "nematocytes genes" gene set, and the 11 categories of gene ontology (filtered data of experiment A). Only genes belonging to one of the 8 pre-defined expression profiles are taken into account in the bar charts. On top of each bar chart: sum of the genes falling into one of these 8 expression profiles, indicated in percentage and in absolute numbers (between parenthesis) with respect to all genes for each gene set.

ORAL maximum of expression



ABORAL maximum of expression

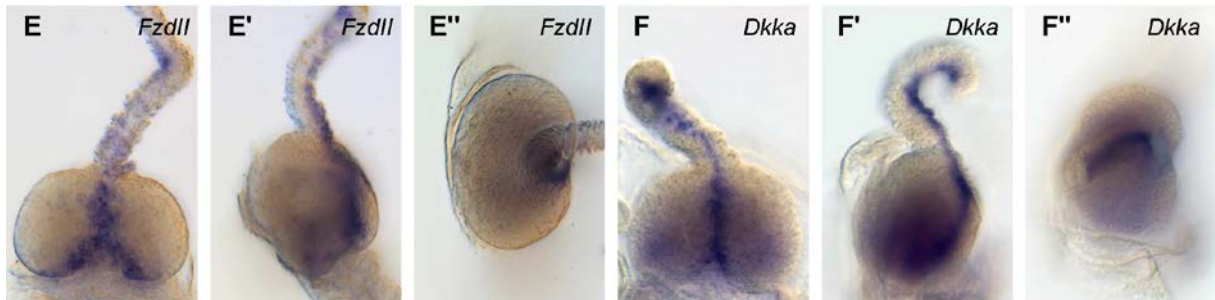


**Fig. 6.** Whole-mount *in situ* hybridisation for Wnt, Fzd and Dkka genes showing a polarized expression along the oral-aboral axis of the bulb. For each gene: left, frontal view (distal pole on top); middle: lateral view (distal pole on top, oral side on the left); right: distal view (oral side on the left).

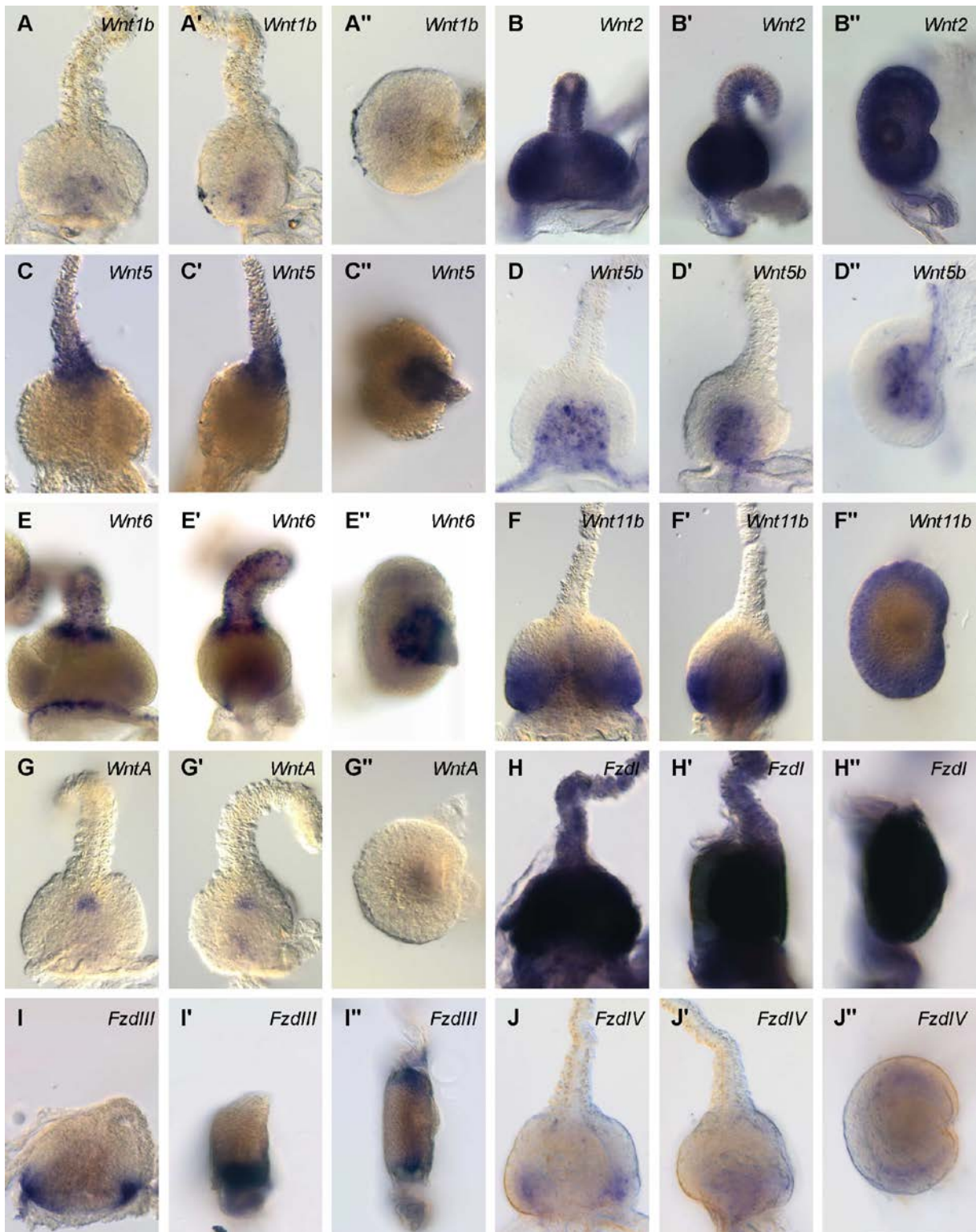


**Fig. 7.** Whole-mount *in situ* hybridisation for the Wnt and Fzd genes not showing polarized expression along the oral-aboral axis of the bulb. For each gene: left, frontal view (distal pole on top); middle: lateral view (distal pole on top, oral side on the left); right: distal view (oral side on the left).